ELSEVIER

Chemical Engineering Journal 135S (2008) S317–S326

Chemical Engineering Journal

www.elsevier.com/locate/cej

Enhancing surface activity in silicon microreactors: Use of black silicon and alumina as catalyst supports for chemical and biological applications

Marilyne Roumanie [a], Cyril Delattre [b,*], Frédérique Mittler [b], Gilles Marchand [b], Valérie Meille [c], Claude de Bellefon [c], Christophe Pijolat [a], Guy Tournier [a], Patrick Pouteau [b]

[a] *Ecole des Mines de Saint Etienne, Centre SPIN, Dpt MICC, LPMG-UMR CNRS 5148, 58 Cours Fauriel, 42023 Saint Etienne, France*
[b] *Laboratoire d'Electronique et de Technologie de l'Information, CEA-LETI/DTBS, 17 rue Martyrs, 38054 Grenoble Cedex 9, France*
[c] *Laboratoire de Génie des Procédés Catalytiques, CNRS-CPE, 43 bd 11 novembre 1918, BP 2077, 69616 Villeurbanne Cedex, France*

Abstract

When surface-supported chemical reactions are performed in microsystems, high production rate cannot be obtained due to the intrinsically low surface area. Increasing the active surface area of silicon microsystems is a challenge that is addressed in this paper using two original approaches: (i) modifying the structure of silicon by creating nanostructures (black silicon) using conventional etching processes of silicon micromachining or (ii) depositing a layer of porous γ-alumina by washcoating a colloidal suspension of boehmite onto the silicon surface. The catalytic oxidation of carbon monoxide on platinum was chosen as a first test reaction in the domain of heterogeneous catalysis. In order to perform this reaction, platinum was either deposited by sputtering on silicon devices with black silicon nanostructuration, or impregnated inside the porosity of an alumina layer previously deposited on a silicon device. For specific biological applications, such as proteins analysis, some biological reactions could be advantageously achieved in microsystems using surface-supported species. As an example, an enzymatic reaction was carried out using silicon devices modified with black silicon nanostructuration and further functionalized with trypsin as a model enzyme. The catalytic activity was compared between silicon devices with the same two types of catalysts, comprising or not an enhancement of the surface activity. A minimum 10-fold increase in catalytic activity was estimated from kinetic measurements and represents the augmentation of the active surface really available for reactions. It was also shown how these catalytic materials were integrated in a microreactor increasing its catalytic active surface without modifying its global size.

Keywords: Microreactor; Catalysis; Black silicon; Washcoat; Alumina; Platinum; Trypsin

1. Introduction

Performing chemical or biological reactions in microsystems, or microreactors, provides well-known advantages such as enhancing the surface to volume ratio [1] leading to fast mass and heat transfer [2], running dangerous reactions under safe conditions [3] or reliably controlling the temperature [4]. Surface-supported catalytic reactions where the catalyst is immobilized inside a reactor are of particular interest in chemical industry because no additional step is needed to separate the catalyst from the chemical products. In chemical research, microreactors designed for running heterogeneous catalysis reaction would be useful for catalyst screening or fine chemical production [5]. For these applications, grafting of catalysts on the microreactor surface is required. The specific surface formed in this way is called an active or a functionalized surface. Its surface area is inherently limited to the surface area of the microreactor walls and can often be too low to ensure a satisfying conversion rate. In order to take full advantage of using microreactors for surface-supported catalytic reactions, surface modifications have already been developed to increase the active surface area without changing the overall size of the microsystem. For heterogeneous catalysis in chemistry, porous materials are usually incorporated inside the microreactor in order to increase the active surface. Main approaches are based on porous pellets of metal oxide [6,7], or porous layer obtained from a colloidal solution of alumina [8,9] or zeolite [10]. Some of these porous materials have an intrinsic catalytic activity, but they can also be impregnated with an active catalytic phase such as metals (e.g. platinum, palladium, nickel). In another scientific area, microreactors with enzymes (natural catalysts involved in most of the biological reactions) grafted on their surface would be essential

* Corresponding author. Tel.: +33 4 3878 2343; fax: +33 4 3878 5787.
E-mail address: cyril.delattre@cea.fr (C. Delattre).

1385-8947/$ – see front matter © 2007 Elsevier B.V. All rights reserved.
doi:10.1016/j.cej.2007.07.053

tools to perform biological reactions, such as proteins digestion [11–13] without loosing the enzyme in the experimental medium or having a reaction of enzyme auto-digestion. Enzymatic reactions have already been performed in microreactor with enzymes grafted on porous silicon matrixes to enhance the surface activity [14]. However, fabricating porous silicon involves a combination of electrochemical and wet chemical processes in fluorohydric acid bath, which can be quite difficult and dangerous. Following the same processes used for metallic heterogeneous catalysis, enzymes have been immobilized on a porous layer of metal oxide (silicalite) in microchannels [15]. For both enzymatic and metallic heterogeneous catalysis, when creation of porosity is needed, working at micrometric size raises new challenges, such as coating channels with micrometric dimensions (less than 10 μm wide), control of deposit homogeneity or compatibility of the deposition processes with the final packaging of the microreactor.

In order to address these issues, we present in this paper two original means of increasing the active surface area of a microsystem: (i) modification of a silicon (Si) device into nanostructured silicon (black silicon) using purely silicon microfabrication processes, followed by platinum (Pt) deposition by sputtering or trypsin grafting; (ii) washcoating porous alumina (Al_2O_3) on a silicon device and impregnation with Pt, using classical methods from the heterogeneous catalysis area. Both of these enhanced active surfaces were fabricated on planar silicon devices and in microsystems containing channels. Two catalytic model reactions (carbon monoxide (CO) oxidation catalyzed by Pt and hydrolysis of α-*N*-benzoyl-L-arginine ethyl ester hydrochloride (BAEE) catalyzed by trypsin) were performed on devices with and without these surface modifications. A catalytic activity for each device was extracted from the kinetic rates. This activity was compared between modified and un-modified devices, leading to an estimation of the enhancement of active surface area.

2. Experimental

2.1. Materials

All reagents used were reagent grade. MilliQ water (18.2 MΩ) was used to prepare aqueous solutions. PBS solution was prepared by dissolving a pellet of PBS (Sigma–Aldrich #1000-3) in 1 L of water. Sodium hydroxide (Sigma–Aldrich #480878), sodium chloride (Sigma–Aldrich #S9888), hydrochloric acid 1N (SDS Solvants #3150015), ethanol (Carlo Erba #414587), toluene (Carlo Erba #488551), 65% nitric acid (Carlo Erba), acetone VLSI (Rockwood Electronic Materials), sodium periodate (Sigma–Aldrich #210048), triethylamine (Sigma–Aldrich #543969), 5,6-epoxyhexyltriethoxysilane (Roth-Sochiel #SIE4675.0), boehmite powder (Disperal, from SASOL Chemie), platinum acetylacetonate (Strem Chemical #78-1400), sodium cyanoborohydride (Sigma–Aldrich #156159), phosphate buffer (Sigma–Aldrich #P5244), Tween 20 (Sigma–Aldrich #P7949), sodium bicarbonate (Sigma–Aldrich #A6141), trypsin (type I extracted from bovine pancreas, Sigma–Aldrich #T8003), biotinylated trypsin (Sigma–Aldrich #T6640), streptavidin carrying Cy3 fluorochrome functions (Sigma–Aldrich #S6402) and α-*N*-benzoyl-L-arginine ethyl ester hydrochloride (Sigma–Aldrich #4500) were used as received.

2.2. Fabrication of silicon devices

Planar and structured devices were fabricated from single crystal silicon wafer (100 mm diameter, 500 μm thickness) with standard processes of silicon microfabrication. First, some planar devices were fabricated by growing a 100 nm silicon oxide (SiO_2) layer (Fig. 1a). SiO_2 was obtained by wet oxidation in a furnace with a steam flow at 1050 °C. This process is completely isotropic and SiO_2 gets deposited on the whole surface of the wafers.

Secondly, structured devices were fabricated using an initial 4 μm thick spin coated photoresist on which a step of photolithography was performed in order to define the pattern of microchannels (Fig. 2a). Using this photoresist layer as an etching mask, deep reactive ion etching (DRIE) was used to etch a 100 μm deep channel in the silicon (Fig. 2b). The DRIE process, also known as Bosch process [16,17], was performed on a STS multiplex machine. This process modifies one side of the wafers only.

The photoresist was then removed in a fuming nitric bath (Fig. 2c) and a 100 nm SiO_2 layer was grown (Fig. 2d).

It was finally possible to bond a Pyrex wafer (Pyrex is trademark from Corning Glass Works Inc.) on top of some wafers using anodic bonding [18,19], thus creating a microreactor with an inlet, an outlet and a reaction area (Fig. 3).

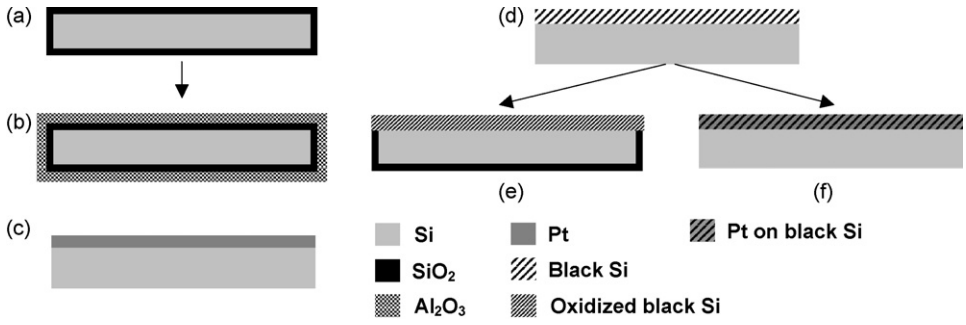

Fig. 1. Schematic diagram of planar devices microfabrication (in transverse section): (a and e) SiO_2 growth; (b) Al_2O_3 washcoating; (c and f) Pt deposition; (d) black silicon formation (see text for details and typical values).

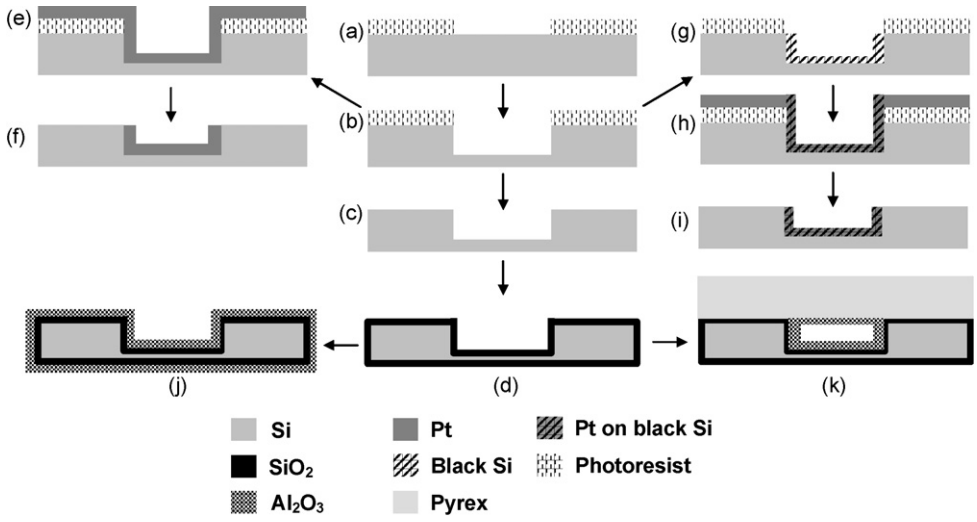

Fig. 2. Schematic diagram of structured devices microfabrication (in transverse section): (a) Photoresist patterning on silicon wafer; (b) DRIE of channels; (c) photoresist removal; (d) SiO_2 growth; (e and h) Pt deposition; (f and I) Pt patterning by photoresist lift-off; (g) black silicon formation; (j) Al_2O_3 washcoating; (k) Al_2O_3 washcoating in bonded oxidized wafer (see text for details and typical values).

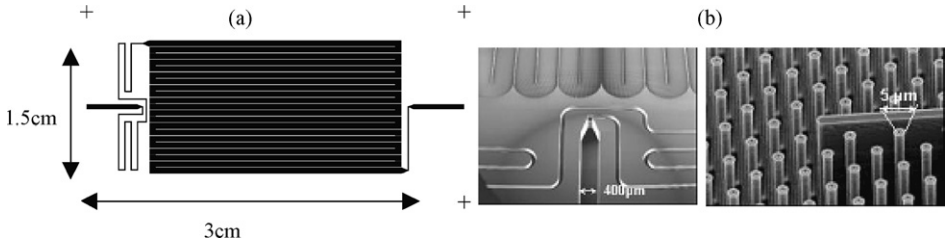

Fig. 3. Schematic presentation of the structured devices (a) and top view scanning electron microscopy (SEM) pictures of the inlet and the pillared structure inside the reaction channels (b).

2.3. Active surface enhancement

2.3.1. Silicon nanostructuration using black silicon

The DRIE of silicon is now a classical technology to create high aspect ratio structures in silicon microsystems. This process was initially developed to produce structures with very high vertical aspect ratio (up to 20). It consists in alternating etching and passivation steps with known duration and frequency. Using a different set of experimental parameters, this process can also generate large area of nanostructured peaks when the passivation gas is in excess during the etching step [20]. This particular silicon nanostructuration is called black silicon, as it will completely inhibit light reflection. It has already been used to generate extremely hydrophobic surfaces [21] or to absorb light for photovoltaic applications [22]. Experimental conditions to get black silicon using a DRIE process have been reported by other research groups [20,23]. Basically, this nanostructured silicon surface consists of silicon peaks spaced at random (Fig. 4A). The geometrical characteristics of the peaks (height, width and angle) largely depend on the experimental conditions. In this paper (Fig. 4B), black silicon was fabricated with the same STS machine used for the DRIE process and these peaks coated with Pt can be represented by sharp and conical features of 1.5 μm height and 0.2 μm width at half-height. The external surface area

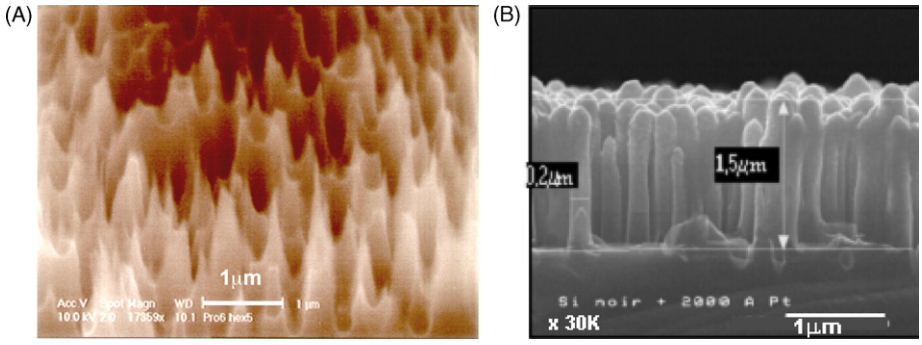

Fig. 4. SEM pictures of black silicon before (A) and after sputtering of a 200 nm layer of Pt (B).

for a single cone with these geometrical features is 1.95 μm^2, when the planar surface area occupied by the same peak is 0.12 μm^2.

The ratio between these two surfaces is equal to 15 and represents the theoretical increase of surface area. If heterogeneous reactions occur on this solid surface and no mass transfer phenomena are involved, the apparent reaction kinetics is directly proportional to the area of active surface and would then be increased by this ratio. Black silicon was fabricated on planar devices starting from blank silicon wafer (Fig. 1d). A 100 nm SiO_2 layer was further grown on some of these devices (Fig. 1e) using the process of Fig. 1a. On structured devices, black silicon was obtained right after DRIE of microchannels (Fig. 2g).

2.3.2. Alumina washcoating

γ-Al_2O_3 is a porous support widely used in catalysis to disperse a nanosized metallic catalyst and thus increase its active surface. Pt supported on Al_2O_3 (Pt/Al_2O_3) is a very classic catalyst, which was synthesized in situ as a thin layer on the silicon devices. The deposition process requires several steps, described in details in a previous work [24] and summarized in this paper. An initial surface activation to create silanol chemical groups on the SiO_2 layer has to be done to ensure that the Al_2O_3 layer sticks to the surface. Two processes were tested and compared by placing devices either in an oxygen plasma reactor (Machine Plassys MDS 150, power 600 W, oxygen flow rate 25 $cm^3\ min^{-1}$, duration 60 s) or in a Brown solution (1 g sodium hydroxide, 3 mL water and 4 mL ethanol) for 2 h at room temperature. The choice between these activation processes depends on the final packaging of the microsystem, e.g. if the Al_2O_3 washcoating has to be performed on non-bonded structured devices, the treatment by oxygen plasma will be chosen. On the contrary, the treatment with a basic solution was preferentially used with microreactor (bonded structured devices). A colloidal boehmite suspension (Al_2O_3 precursor) was then prepared by dispersing a boehmite powder at a concentration of 20 g L^{-1} in a nitric acid solution, leading to an aqueous solution with a resulting pH around 3. Next, the devices were washcoated with the suspension either by dip coating (Figs. 1b and 2j), or by circulating the suspension in the microreactor (Fig. 2k). The devices were subsequently calcinated at 600 °C under air to obtain the γ-crystalline form of Al_2O_3.

2.4. Devices functionalization

Starting from the devices with enhanced active surface, chemical functions were added on the surface to provide heterogeneous catalytic activity (metallic or enzymatic): (i) platinum deposition, (ii) platinum impregnation in alumina washcoating, and (iii) trypsin grafting.

2.4.1. Platinum deposition

A process of cathodic sputtering was carried out for Pt deposition on one side of the wafers only. On planar devices, a 200 nm Pt layer was deposited either on blank silicon wafers (Fig. 1c), or on silicon wafers with black silicon (Fig. 1f), creating functionalized planar devices called, respectively, P-Pt and P-bSi-Pt. On a first type of structured devices, a 200 nm Pt layer was deposited after DRIE the process (Fig. 2e). The photoresist was then removed in a fuming nitric bath (Fig. 2f), localizing the Pt layer only in the channels by lift-off (devices S-Pt). On a second type of structured devices, a cleaning step for 10 min in buffered oxide etch solution (BOE) was done after black silicon formation to remove any fluoro-polymers deposited during this last process. A 200 nm Pt layer was then deposited (Fig. 2h). Finally, the photoresist was removed in a fuming nitric bath (Fig. 2i) to localize the Pt layer by lift-off (devices S-bSi-Pt).

2.4.2. Platinum impregnation on alumina washcoating

Starting from the planar and structured devices washcoated with an Al_2O_3 layer (Figs. 1b and 2j and k), Pt was impregnated into this porous layer with a solution of platinum acetylacetonate in toluene (either by dip-coating or circulating the solution). These devices were finally calcinated at 400 °C under air. They will further be called P-Al-Pt for planar devices, S-Al-Pt for structured devices and S-Al-Pt-bonded for microreactor.

2.4.3. Trypsin grafting

Starting from planar devices with a SiO_2 layer grown on a blank wafer or on a black silicon surface (Fig. 1a and e), grafting of trypsin enzyme on the devices was achieved in four steps: (i) SiO_2 hydratation, (ii) silanization, (iii) modification of a chemical group of the silane molecule and (iv) trypsin immobilization. (i) Hydratation of SiO_2 surface was obtained by incubation of the devices during 2 h at room temperature in Brown solution in order to generate silanol groups on the surface. The devices were then washed with water and dried under nitrogen flow. (ii) The silane 5,6-epoxyhexyltriethoxysilane was grafted on the surface using a mixture of toluene, triethylamine and silane (20 mL/100 μL/50 μL) at room temperature during 24 h. The devices were successively rinsed with ethanol and water, and dried under nitrogen flow. They were finally baked during 3 h at 110 °C. (iii) The terminal epoxide group on the silane was modified to create a diol chemical group by treating the devices in an aqueous solution of hydrochloric acid at 0.2 mol L^{-1} during 3 h at room temperature. The devices were abundantly washed with water and dried under nitrogen flow. Oxidation of the diol function to obtain an aldehyde function was performed in an aqueous solution of sodium periodate and water (220 mg/10 mL) during 1 h at room temperature. The devices were finally washed with water and dried under nitrogen flow. (iv) Immobilization of trypsin was obtained by covalently linking some amines groups (lysine) of the enzyme to the aldehyde group of the silane. The devices were immersed in a mixture formed by 4.5 mL of water, 2.25 mL of phosphate buffer at 0.1 mol L^{-1}, 2.25 mL of an aqueous solution of sodium cyanoborohydride at 0.05 mol L^{-1} and 11 mg of trypsin, during 20 h at 4 °C. A first rinsing step was performed using a mixture formed by 450 mL of PBS solution, 50 mL of an aqueous solution of sodium chloride at 0.5 mol L^{-1} and 250 μL of Tween 20. A second rinsing step was achieved using the PBS solution only. The devices were finally stored at 4 °C in the PBS solution. Devices without and with black

Table 1
Silicon devices and materials at their surface

Planar substrates		Structured substrates	
References	Material	References	Material
P-Pt	Pt	S-Pt	Pt
P-bSi-Pt	Black silicon and Pt	S-bSi-Pt	Black silicon and Pt
P-Al-Pt	Al_2O_3 and Pt	S-Al-Pt	Al_2O_3 and Pt
P-Tryp	Trypsin	S-Al-Pt-bonded	Al_2O_3 and Pt
P-bSi-Tryp	Black silicon and trypsin		

silicon nanostructuration were respectively named P-Tryp and P-bSi-Tryp.

All the wafers previously described (bonded or not) were diced at various dimensions for future testing. For a purpose of clarity, all the devices and the materials at their surface are listed in Table 1.

3. Characterization of functionalized devices

Multiple characterization means were used to obtain data on the following items: black silicon formation and platinum deposition inside microchannels (particularly on the walls), effect of surface activation and solution aging on alumina washcoating, alumina washcoating inside microchannels and trypsin grafting.

3.1. Black silicon and platinum deposition

On planar devices P-bSi-Pt, the SEM pictures in Fig. 4 gives clear evidence of black silicon formation and efficient Pt deposition. The peaks were rounded because of the Pt layer. For structured devices S-Pt and S-bSi-Pt, SEM pictures clearly show that nanostructures were obtained on the vertical wall of the pillars during black silicon formation (Fig. 5). For the devices S-Pt without black silicon (Fig. 5, panel 1), the steps and scales observed respectively on the top view and on the bottom view come from the DRIE process used for fabrication. Black silicon on devices S-bSi-Pt is characterized on pillar wall by pores of roughly 0.3 μm diameter and on the channel bottom by peaks similar to those obtained on a planar device (Fig. 5, panel 2). This topography is of particular interest for catalytic applications because, for a given microsystem surface area, the active surface of the catalyst will be increased.

From these SEM pictures, the Pt layer cannot be seen in the microchannels. Other analytical means were used such as an elementary analysis using an energy dispersive X-ray probe. This method gave confirmation that Pt was deposited on the channel bottom. Furthermore, a structured device was calcinated at 600 °C and Pt crystallites were observed on the top of the pillars by SEM after this sintering step. These experiments clearly revealed qualitatively that more Pt is deposited on the pillar top than on the pillar bottom. In conclusion, all these results show that Pt was deposited both on pillar wall and on channel bot-

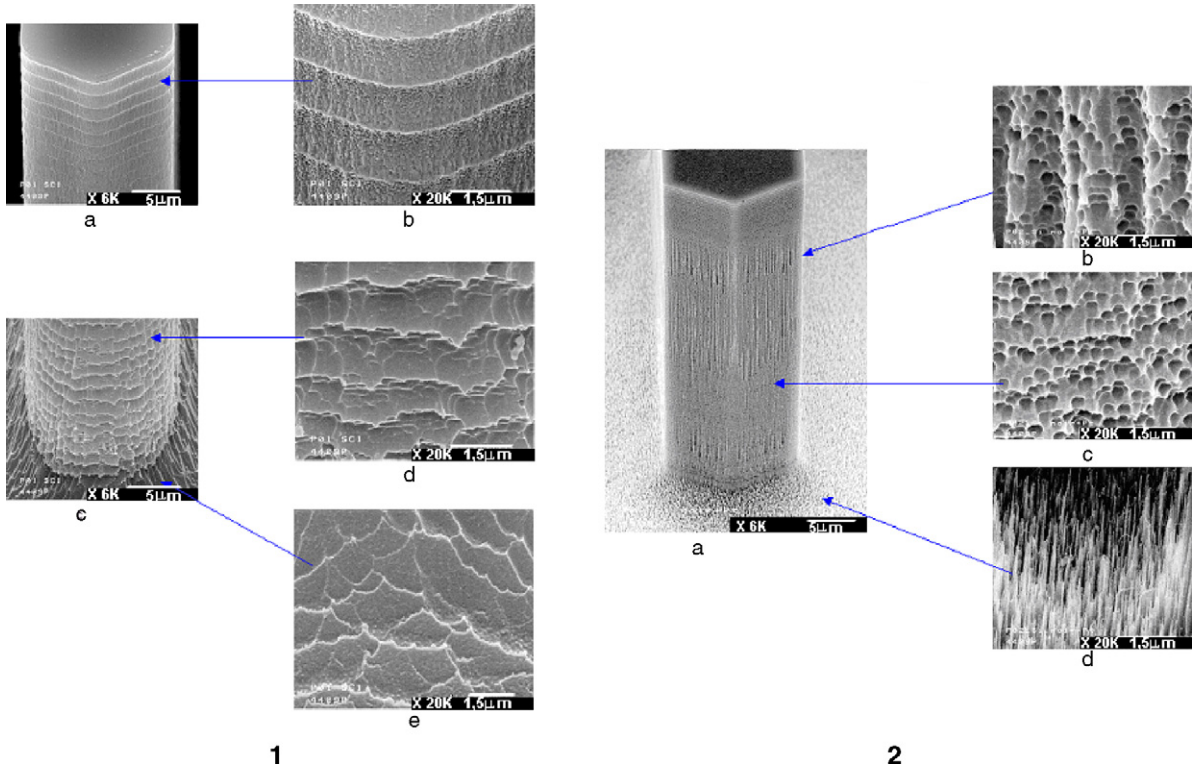

Fig. 5. SEM pictures of a silicon pillar covered with a 200 nm sputtered Pt layer. (1) Devices S-Pt (without black silicon): (a) pillar top view; (b) enlargement of the top view; (c) pillar bottom view; (d and e) enlargements of the bottom view. (2) Devices S-bSi-Pt (with black silicon): (a) pillar view; (b and c) enlargements of the pillar top view and bottom view; (d) enlargement of the channel bottom view.

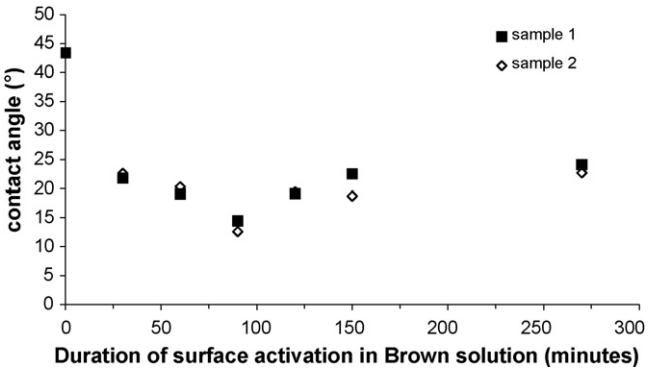

Fig. 6. Influence of the activation time with Brown solution on the contact angle of the boehmite suspension on a planar device with a SiO_2 layer.

tom, thanks to the sputtering process that is a non-directional physical deposition process, leading to a good surface coverage. However, the lack of uniformity of the Pt coverage is due to the high aspect ratio of the pillar limiting the deposition on pillar bottom.

3.2. Alumina washcoating on planar devices

The influence of the surface activation process was studied in terms of surface wettability, by measuring the wetting contact angle that represents the capability of a liquid to spread on a surface. Contact angle measurements between the boehmite solution and a planar device with a SiO_2 layer (Fig. 1a) were achieved using a Digidrop system (GBX, France). Without applying any surface activation processes, the contact angle is close to 44°. The oxygen plasma process leads to the complete spreading of the droplet on the surface with a contact angle below 10°. On the contrary, when the Brown solution is used for activation, the wetting angle decreases very quickly with the duration of activation to reach 20° after 30 min and stabilizes at this value (Fig. 6). Complete spreading was never observed. Two samples were measured using the same procedure and the results show a very good reproducibility.

To conclude, the oxygen plasma treatment is the most efficient method to create a highly wettable SiO_2 surface for the boehmite solution. However, this process cannot be used for bonded structured devices. In this case, the activation by a Brown solution leads to a sufficiently low contact angle to ensure an efficient washcoating process, which was demonstrated by running successfully catalytic tests on these devices.

Table 2
Evolution of pH and viscosity of the boehmite solution (viscosity measurements were performed with a capillary viscosimeter)

	pH	Viscosity (mPa s)
Initial suspension	2.5	1.1
Suspension after 2 years	6	2.5

3.2.1. Thickness and topography of the alumina layer

An Al_2O_3 layer was obtained on planar devices following the experimental procedure previously described, using in particular an oxygen plasma for surface activation and a dip coating process for suspension deposition. Different devices were produced using two boehmite suspensions: a freshly prepared mixture, named initial suspension, and a suspension prepared 2 years before. pH value and dynamic viscosity were measured for both suspensions (Table 2).

The suspension (sol) behaves initially as a Newtonian fluid. Then, by a slow phenomenon over time, it becomes a gel with an increasing viscosity and a decreasing pH. As the thickness and the topography of the Al_2O_3 layer will depend on the viscosity of the suspension, atomic force microscopy (multimode scanning probe/digital instruments) was used in contact mode in order to characterize these two parameters. The AFM data were recorded on different places of the sample surface and each time on a 2500 μm^2 area. A step between the silicon device and the Al_2O_3 layer was created using a scotch tape during washcoating (Fig. 7a).

The thickness of the layer was then easily measured and a value around 0.5 μm was obtained for the device washcoated with the aged suspension (2 years). When the initial suspension was used for washcoating, the thickness was an order of magnitude lower, clearly showing an effect of the suspension viscosity. Fore both suspensions, the surface topography appears homogeneous showing no apparent cracks or local lack of Al_2O_3 (Fig. 7b), with localized asperities around 100 nm high. These characterizations were performed on planar silicon devices because it is difficult or impossible to characterize a nanometric layer inside the microchannels of a structured device. The boehmite suspension and, later, the Pt solution were circulated inside the microchannels of bonded structured devices

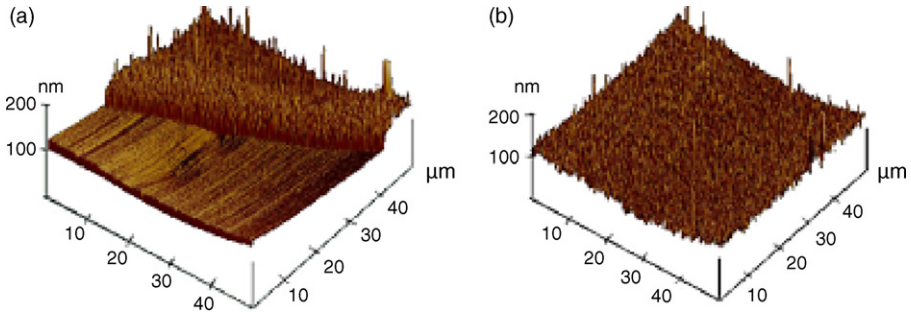

Fig. 7. AFM pictures of an Al_2O_3 layer deposited on device S-Al-Pt initially activated by oxygen plasma: (a) Al_2O_3 step on oxidized silicon and (b) Al_2O_3 layer.

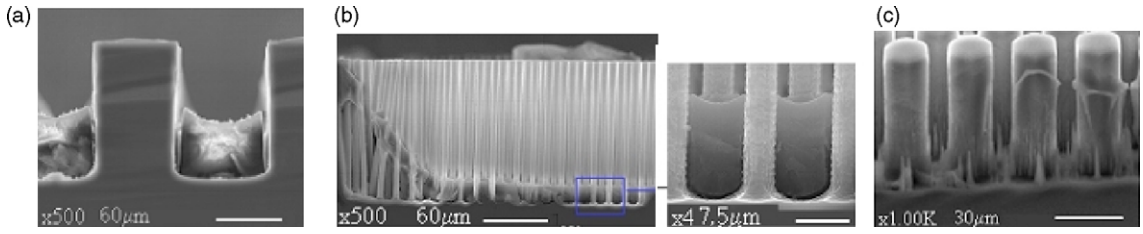

Fig. 8. SEM pictures of an Al_2O_3 washcoat in structured devices: (a) without a SiO_2 layer with activation, (b) with a SiO_2 layer without activation, and (c) with a SiO_2 layer with activation.

(S-Al-Pt-bonded). The presence of catalyst was ultimately verified by running the catalytic tests.

3.3. Alumina washcoating in structured devices

The Al_2O_3 washcoat was deposited by dip coating on structured devices under various experimental conditions and localization of alumina was obtained from SEM pictures (Fig. 8). First of all, a specific device without SiO_2 layer (Fig. 2c) was activated using the oxygen plasma process. The Al_2O_3 crystallites have fallen down to the channel bottom and were not deposited on the microchannel walls (Fig. 8a). In the second case, a device with SiO_2 layer (Fig. 2d) was used without prior surface activation. The Al_2O_3 layer is again observed on the bottom of the channel (Fig. 8b). Finally, an identical device was activated using an oxygen plasma process. In this case, the Al_2O_3 layer seems to be homogeneously deposited on the pillars inside the microchannel (Fig. 8c). In conclusion, both a SiO_2 layer and its activation are two essential conditions for the Al_2O_3 layer to adhere on the surface of the pillars.

Noticeably, using this washcoating method, an Al_2O_3 layer is also deposited on every elevated surface of the device. However, when capped microchannels are needed, a very low surface roughness is necessary for direct anodic bonding with a Pyrex cover (generally ~1.5 nm). A polishing step would thus be necessary, but involves some clogging risks for the microchannels. For this reason, Al_2O_3 washcoating was performed on bonded structured devices by circulating the boehmite suspension through the microchannels. Further characterization for these particular devices was previously described [24].

3.4. Trypsin immobilization

Biotinylated trypsin was grafted on the SiO_2 surface of a planar device following the procedure described previously. The only change occurred during the immobilization step, in which the trypsin solution was selectively deposited on the surface as a droplet. Following the second rinsing step, the device was incubated in a solution prepared by dissolving 2 μL of streptavidin protein carrying Cy3 fluorochrome functions in 80 μL of a buffer solution (based on PBS solution at pH 7.4, Tween 20 at 0.05% and NaCl at 1 M) for 15 min at room temperature with no external light. Biotin and streptavidin are widely used in molecular recognition mechanisms because of their complementary binding sites. Consequently, wherever the biotinylated trypsin is immobilized, the streptavidin will be linked specifically. The surface was first rinsed for 5 min with the buffer solution and finally for 5 min with PBS solution only. The device was subsequently dried under nitrogen flow and a fluorescence microscope was used to obtain a fluorescence image. A bright spot within a black area was observed. This spot coincides with the footprint of the droplet of trypsin solution, showing that trypsin was successfully and selectively immobilized on the surface. However, the catalytic activity of the immobilized trypsin can only be characterized by running biological reactions.

4. Catalytic tests and discussion

4.1. Platinum-catalyzed reaction on planar devices

CO oxidation was chosen as a model reaction to compare the activity of three Pt-based catalysts (P-Pt, P-bSi-Pt, and P-Al-Pt). This reaction is well-documented and relatively easy to carry out. Catalysts were prepared as described on planar devices, which were diced into small pieces (1 mm^2) to fit the dimensions of a catalytic fixed bed reactor. This reactor was composed of a quartz tube (0.8 cm internal diameter and 24.5 cm length) placed in a tubular oven. The calaytic pieces (2 g) were placed in the middle of the tube on a sintered quartz support, creating a packed bed 1.5 cm high. A mixture of CO at 300 ppm in air was injected at the inlet with a flow rate of 3 L/h controlled with a mass flow meter. An infrared analyzer (URAS 10) was installed at the outlet giving continuously access to the composition of the gas phase, by analyzing carbon monoxide and carbon dioxide (CO_2). The furnace temperature and data from the IR analyzer were recorded with a homemade software build with the LABVIEW® software. The CO conversion was calculated from the measurements of CO and CO_2 concentrations and its evolution was plotted as the temperature is increased starting from room temperature (Fig. 9). The CO oxidation is a very exothermic reaction and a well-known light-off phenomenon was observed, showing a sharp increase of CO conversion up to almost total conversion for a given temperature, called ignition temperature. For a given reactor, the value of the ignition temperature is inversely related to the quantity of active catalyst or its intrinsic activity.

In this paper, the ignition temperature was determined at 10% conversion and was used to compare the catalysts activity (Table 3). Pt was also deposited with a thickness of 20 nm on planar devices P-Pt. These catalysts were also tested and no apparent effect of the Pt layer thickness on the ignition temperature was observed. This shows that CO oxidation occurs preferentially at the surface of the Pt layer and not in the bulk.

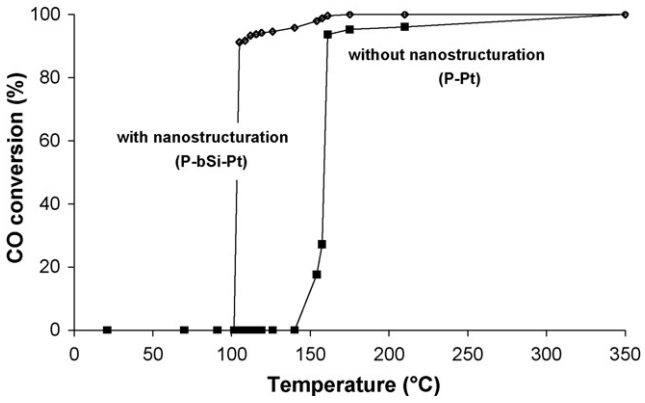

Fig. 9. CO conversion vs. temperature curve for planar silicon devices with 200 nm of platinum.

Therefore, the active surface can be represented by the geometric surface of the Pt layer.

For the particular case in Fig. 9, the ignition temperature decreases when nanostructured devices were used. As the thickness of the Pt layer has no effect on the catalyst activity and the chemical nature of the support is identical (e.g. silicon), the only changing parameter between the devices is the surface nanostructuration. Black silicon structuration increases the active surface area and thus the quantity of active catalyst available for the reaction, without changing the overall quantity of silicon device. The increase of the active surface area due to the black silicon structuration was estimated from ignition temperature values, using the following argument. Using a Langmuir–Hinshelwood mechanism, the CO oxidation kinetic rate can be written as

$$R = \frac{k_T C_{O_2} C_{CO}}{(1 + K_T C_{CO})^2} \quad (1)$$

where k_T is a kinetic constant linearly linked to both the intrinsic kinetic constant and the global active surface area of catalyst inside the reactor S_a, and K_T is the equilibrium constant for CO adsorption [25]. Variation of these two constants with the reactor temperature can be described by an Arrhenius function, such as $k = A\,e^{-E/RT}$, where A is a pre-exponential factor and E is respectively the activation energy (E_a) for k_T and the adsorption enthalpy (ΔH_{ads}) for K_T. At low conversion (less than 10%) and in absence of mass transfer bias, the conversion is directly proportional to the kinetic rate. As total CO conversion is always reached when the temperature is increased, it can be assumed that no mass transfer limitations occur in our system [26]. Two catalysts with different surface activity placed in the same reactor would lead to an identical CO conversion (e.g. an identical kinetic rate) but for different temperatures. In this case, the following equation can then be derived from equation (1):

$$\frac{k_{T_1}}{(1 + K_{T_1} C_{CO})^2} = \frac{k_{T_2}}{(1 + K_{T_2} C_{CO})^2} \quad (2)$$

Considering the two extreme cases $K_T C_{CO} \gg 1$ or $K_T C_{CO} \ll 1$, the ratio between two active surfaces can then be estimated within an interval using

$$e^{(E_a/R)(1/T_1 - 1/T_2)} \leq \frac{S_{a1}}{S_{a2}} \leq e^{((E_a - 2\Delta H_{ads})/R)(1/T_1 - 1/T_2)} \quad (3)$$

with the assumption that the active sites of Pt stay unchanged when it is deposited on black silicon, the active surface being the only varying parameter. With average values of 80 kJ mol^{-1} for E_a and -3.127 kJ mol^{-1} for ΔH_{ads} [25,27], this ratio is then restricted to

$$10 \leq \frac{S_{a\ P-bSi-Pt\,(102\,^\circ C)}}{S_{a\ P-Pt\,(147\,^\circ C)}} \leq 20 \quad (4)$$

This ratio is in very good agreement with the theoretical value previously estimated from a geometrical point of view.

A major gap of 80 °C in the ignition temperatures was observed between devices with sputtered Pt and those with Pt impregnated in Al_2O_3, showing that P-Al-Pt catalysts were far more active than P-bSi-Pt. Pt content on both devices was measured by ICP analysis after complete dissolution of the devices. Ten times more Pt is present on the device with Al_2O_3 than on the black silicon device. However, this difference in quantity of metallic Pt is not sufficiently large to explain the gap between the values of ignition temperature. An additional difference in catalyst activity could arise during the catalyst fabrication process as sputtered Pt is deposited as a continuous thin film on the device surface, whereas for the P-Al-Pt catalyst, well-dispersed crystallites of Pt are created inside Al_2O_3 porosity, leading to a higher activity for CO oxidation. From an industrial perspective, silicon microsystems with Pt impregnated in porous Al_2O_3 will lead to a high production rate for a small overall volume. However, deposition of the catalyst inside a microstructure involves several fabrication steps (surface activation, washcoating, drying, calcinations, impregnation). On the opposite, processes for black silicon formation and Pt sputtering are fairly easy to integrate in a microreactor fabrication process and the enhancement of surface activity could be sufficient for some applications.

Table 3
Ignition temperature for different catalysts

Catalysts	$T_{ignition}$ (°C)	Activity
P-Pt (200 nm)	147	
P-bSi-Pt (200 nm)	102	
P-bSi-Pt (20 nm)	100	
P-Al-Pt	25	

4.2. Platinum-catalyzed reaction in bonded structured devices

The CO oxidation was tested with devices S-Al-Pt-bonded (Al_2O_3 washcoating and Pt impregnation) and an ignition temperature of 30 °C was observed (Fig. 10). This result is close to the ignition temperature obtained during the previous tests achieved in macroreactor with the same catalyst on planar devices. At low conversion, the activation energy can readily be obtained by plotting the conversion versus the inverse of temperature. A value of 78 kJ mol^{-1} was calculated, in good agreement

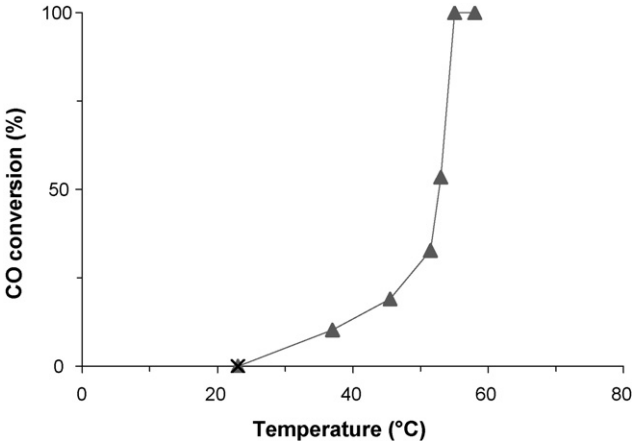

Fig. 10. CO conversion vs. temperature curve for a device S-Al-Pt-bonded with a washcoated Al_2O_3 layer impregnated with Pt.

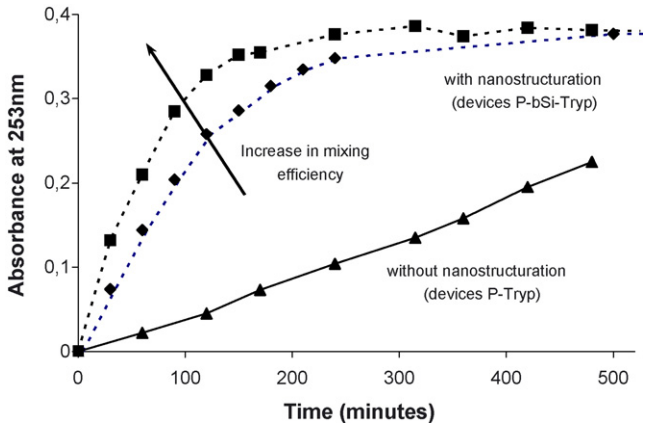

Fig. 11. Absorbance of BA produced from BAEE digestion by trypsin grafted on planar devices.

with published values obtained for a packed-bed microreactor with 1 wt.% Pt/Al_2O_3 catalysts (83.6 kJ mol^{-1}) [25]. All these results show that the Al_2O_3 washcoating and the Pt impregnation were successfully realized in closed microchannels, retaining a complete catalytic activity.

4.3. Trypsin-catalyzed reaction on planar devices

The catalytic activity of grafted trypsin was estimated by following the kinetic rate of the hydrolysis reaction of the BAEE into α-*N*-benzoyl-L-arginine (BA) and ethanol. A BAEE solution concentrated at 0.4 mM was prepared by dissolving BAEE in a solution of sodium bicarbonate at 25 mM in water. Devices P-Tryp and P-bSi-Tryp were diced in square of 4 cm^2 and placed in 17 mL of this solution under constant stirring and room temperature. Five hundred microliters samplings were analyzed at fixed time and the BA concentration was measured with a UV spectrometer at 253 nm. Trypsin leaching from the surface or mechanical damage to the active layer could occur over the experiments. The BA solution obtained at the end of some experiments was analyzed by mass spectrometry. Trypsin was never detected indicating that the grafting process is highly efficient. Moreover, the same devices were used four times over 1-month period, using the storage conditions as described in the experimental section. The repeatability of the experimental data was excellent (within an experimental error of less than 10%, estimated from the ratio between the standard deviation to the average value), showing no loss in the catalytic activity of trypsin. The reaction rate for this reaction can be accurately described by the Michaelis–Menten equation [28]. At first, Michaelis–Menten parameters for trypsin grafted on P-Tryp devices were determined using initial reaction rates measurements with different BAEE concentrations ($K_m \sim 0.17$ mM and $V_{max} \sim 0.95$ μM/min). The Lineweaver–Burk plot was linear, indicating no apparent mass transfer limitations to the kinetic measurements. These data are consistent with values from previous works [29]. The BA concentration was then recorded over time until complete depletion of BAEE for both devices P-Tryp and P-bSi-Tryp (Fig. 11).

Table 4
Kinetic parameters of Michaelis–Menten equation for planar devices with and without nanostructuration (planar devices)

Devices	K_m (mM)	V_{max} ($\times 10^{-3}$ mM/min)
Initial reaction rates method		
P-Tryp	0.17	0.95
Numerical method		
P-Tryp	0.21	1.1
P-bSi-Tryp (fast agitation)	0.21	6.5
P-bSi-Tryp (slow agitation)	0.36	6

Assuming perfect mixing of the solution during reaction, these data were fitted with Michaelis–Menten model using a numerical method and another set of parameters was obtained (Table 4). The values of the kinetic parameters obtained by both methods for planar devices without nanostructuration were in very good agreement.

It was found that when the mixing efficiency was increased (by increasing the stirring speed) the average kinetic rate for device P-bSi-Tryp increased up to a limit. It clearly indicates that the kinetic data were biased by external diffusional limitations at low mixing efficiency. K_m increases in this case as it was previously reported [29]. This phenomenon did not occur for devices P-Tryp because the active surface is not large enough and the catalytic transformation is still the rate-limiting step in the overall process. Considering that only one face of the device has nanostructuration and that the trypsin density at atomic scale on solid surface is identical between devices with or without nanostructuration, the increase in V_{max} is linearly related to the increase in surface area brought by nanostructuration. This enhancement can be estimated to 11, a value comparable to that obtained for the CO oxidation reaction.

5. Conclusion

Two original ways of increasing the active surface area of a silicon microsystem without changing its overall dimensions were demonstrated. First, nanostructuration (called black silicon) of the silicon surface was fabricated on both planar and

structured devices comprising microchannels. Catalysts were immobilized on the surface: Pt for heterogeneous catalysis applications and trypsin for enzymatic reactions. Kinetic data obtained on devices with and without black silicon nanostructuration were compared. Amplification of the surface activity by a factor of at least 10 was measured. This enhancement was only estimated from experimental results and represents the increase of active surface really available for chemical and biological molecules. Secondly, an alumina layer was deposited using a washcoating process, which was characterized in order to identify the essential parameters such as the activation process or the nature of the surface. The catalytic surface activity was greatly increased in comparison with black silicon structuration. This approach would then be particularly suitable for applications demanding a very high catalyst activity and for which the active surface provided by the black silicon structuration is not sufficient. However, integration of the alumina layer inside closed microchannels could be challenging compared with the simplicity of black silicon fabrication using standard silicon micromachining tools, fully compatible with the rest of the fabrication process.

References

[1] A. de Mello, R. Wootton, Lab Chip 2 (2002) 7N–13N.
[2] H. Löwe, W. Ehrfeld, Electrochim. Acta 44 (1999) 3679–3689.
[3] T.M.T. Janicke, H. Kestenbaum, U. Hagendorf, F. Schüth, M. Fichtner, K. Schubert, J. Catal. 191 (2000) 282–293.
[4] G. Veser, Chem. Eng. Sci. 56 (2001) 1265–1273.
[5] K.F. Jensen, Chem. Eng. Sci. 56 (2001) 293–303.
[6] S.K. Ajmera, M.W. Losey, K.F. Jensen, AIChE J. 47 (2001) 1639–1647.
[7] M.W. Losey, M.A. Schmidt, K.F. Jensen, Ind. Eng. Chem. Res. 40 (2001) 2555–2562.
[8] L.R. Arana, S.B. Schaevitz, A.J. Franz, K.F. Jensen, M.A. Schmidt, J. Microelectromech. Syst. 12 (2003) 1–13.
[9] J. Bravo, A. Karim, T. Conant, G.P. Lopez, A. Datye, Chem. Eng. J. 101 (2004) 113–121.
[10] E.V. Rebrov, G.B.F. Seijger, H.P.A. Calis, M.H.J.M. de Croon, C.M. van den Bleek, J.C. Schouten, Appl. Catal. A 206 (2001) 125–143.
[11] N. Sarrut, S. Bouffet, F. Mittler, O. Constantin, P. Combette, J. Sudor, F. Ricoul, F. Vinet, J. Garin, C. Vauchier, Proceedings of SPIE, vol. 5718: Microfluidics, BioMEMS and Medical Microsystems III, January 2005, pp. 99–109.
[12] S. Ekström, P. Önnerfjord, J. Nilsson, M. Bengtsson, T. Laurell, G. Marko-Varga, Anal. Chem. 72 (2000) 286–293.
[13] K. Sakai-Kato, M. Kato, T. Toyo'oka, Anal. Chem. 75 (2003) 388–393.
[14] J. Drott, K. Lindström, L. Rosengren, T. Laurell, J. Micromech. Microeng. 7 (1997) 14–23.
[15] Y. Huang, W. Shan, B. Liu, Y. Liu, Y. Zhang, Y. Zhao, H. Lu, Y. Tang, P. Yang, Lab Chip 6 (2006) 534.
[16] J. Bhardwaj, H. Ashraf, A. McQuarrie, Proceedings of the Symposium on Microstructures and Microfabricated Systems at the Annual Meeting of the Electrochemical Society, Montreal, Quebec, Canada, May 4–9, 1997.
[17] A.A. Ayon, R. Braff, C.C. Lin, H.H. Sawin, M.A. Schmidt, J. Electrochem. Soc. 146 (1999) 339–349.
[18] D.-J. Lee, B.-K. Ju, J.J. Kwang-Bae Lee, M.-H. Oh, J. Micromech. Microeng. 9 (1999) 313–318.
[19] G. Wallis, D.I. Pomerantz, J. Appl. Phys. 40 (1968) 3946–3949.
[20] H. Jansen, M. De Boer, R. Legtenberg, M. Elwenspoek, J. Micromech. Microeng. 5 (1995) 115–120.
[21] J. Kim, C.J. Kim, Proceedings of the 15th IEEE International Conference on Micro Electro Mechanical Systems, Las Vegas, NV, USA, 2002, pp. 479–482.
[22] M. Schnell, R. Lüdemann, S. Schaefer, Proceedings of the 28th IEEE Photovoltaic Specialists Conference, Anchorage, September 19–22, 2000, pp. 367–370.
[23] R.S. Besser, W.C. Shin, J. Vac. Sci. Technol. B 21 (2003) 912–915.
[24] M. Roumanie, V. Meille, C. Pijolat, G. Tournier, C. de Bellefon, P. Pouteau, C. Delattre, Catal. Today 110 (2005) 164–170.
[25] S.K. Ajmera, C. Delattre, M.A. Schmidt, K.F. Jensen, J. Catal. 209 (2002) 401–412.
[26] F. Duprat, Chem. Eng. Sci. 57 (2002) 901–911.
[27] R.H. Venderbosch, W. Prins, W.P.M. van Swaaij, Chem. Eng. Sci. 53 (1998) 3355–3666.
[28] R.H. Perry, D.W. Green, Perry's Chemical Engineer's Handbook, McGraw-Hill, 1999, p. 21 (Chapter 24).
[29] P.S. Sears, D.S. Clark, Biotechnol. Bioeng. 42 (1993) 118–124.